UDC 538.911

CRYSTAL STRUCTURE OF STRONGLY COUPLED ONE-COMPONENT PLASMAS CONFINED IN QUASI-TWO-DIMENSIONAL GEOMETRY. A MONTE CARLO STUDY

O. V. BYSTRENKO

Bogolyubov Institute for Theoretical Physics, Nat. Acad. Sci. of Ukraine
(14b, Metrolohichna Str., Kyiv 03143, Ukraine)

Strongly coupled one-component plasmas confined in a quasi-two-dimensional geometry are investigated by means of Monte Carlo (MC) computer simulations. The structure of the layers occuring in these systems is studied in terms of the two-dimensional radial pair intra- and interlayer distributions and bond-orientational order parameters. The most remarkable finding is a series of structural transitions with the alternating square (body-centered cubic) and hexagonal (face-centered cubic or hexagonal closely packed) symmetries, as dependent on the interlayer separation. The results of simulations correlate well with the experimental observations of similar transitions in one-dimensionally confined charged colloids and ions in Penning traps.

Introduction

Two-dimensional ($2D$) and quasi-two-dimensional (quasi-$2D$) strongly coupled Coulomb systems attracted considerable attention of researchers during decades. The well-known examples are charged colloids confined between two plates, dusty plasmas trapped in one-dimensional potential profiles, electron plasmas in the inversion layers and quantum wells in semiconductors, etc. [1–5]. Most interesting feature of these systems is their capability to form a strongly correlated condensed state at sufficiently strong coupling (i.e., at low temperatures and high densities), in particular, various crystal structures.

The simplest theoretical model for strongly coupled Coulomb systems is the model of one-component plasmas (OCP). The latter is suitable in the cases where the properties of a system are determined predominantly by the subsystem of charges of one kind, and the effects produced by the other components (e.g., screening) are negligible. In other words, in OCP, only one kind of charges is dynamically or statistically taken into account, while the rest of charges is considered as the immobile neutralizing background.

The properties of infinite three-dimensional ($3D$) OCP are known rather well due to extensive computer simulations [6,7]. It has been established that, for strong coupling, i.e., as the coupling constant exceeds the melting point $\Gamma_m \simeq 178$, OCP freezes in the body-centered cubic (BCC) lattice. Computer simulations of strictly $2D$ OCP have revealed the hexagonal (triangular) type of $2D$ lattice [8,9] with the $2D$ melting point $\Gamma_m \simeq 125$ consistent with the experiments on the melting of $2D$ Coulomb lattice formed by electrons on the surface of liquid helium [10].

At the same time, the detailed structure of strongly coupled OCP in quasi-$2D$ case, i.e., with the deviation from a strictly $2D$ geometry, remains an open question up to now. Theoretical estimates obtained by minimizing the energy (i.e., for zero temperature) evaluated within the fluid theory with keeping the local density correlations, predict a possibility of structural transitions with increasing the system width [11]. Similar transitions with alternating square and hexagonal symmetries have been observed in computer simulations of one-dimensionally ($1D$) confined hard spheres [12]

and in the experiments with charged colloids confined between two plates [1] and with planar ion structures in Penning traps [13]. However, a direct numerical evidence based on microscopic computer simulations which could confirm the above assumption, is missing up to now. Molecular dynamics simulations for $1D$-confined OCP have revealed only the regular triangular type of an intralayer structure in multilayered Coulomb systems [14].

The goal of this work is to study the crystal structure of $1D$-confined strongly coupled OCP by means of precise microscopic Monte Carlo (MC) simulations, in particular, to answer the above question about a possibility of structural transitions with alternating symmetry in this system.

1. Calculation of the Coulomb Energy in Quasi-two-dimensional Systems

In computer simulations of Coulomb systems, one of the most difficult problems is to combine the periodic boundary conditions with the long-range Coulomb interactions between particles. In order to tackle this problem, we employ the method developed in [15] for two-component plasmas.

Let us examine a one-dimensionally (along the Z-axis) confined Coulomb system consisting of point-like charges of one kind (each carrying a charge Q) in the immobile neutralizing background. The simplest case related to a quasi-$2D$ geometry is that the background is uniform and occupies a volume of finite width in the Z-direction ($-H < Z < H$) and infinite in the XY-directions. Following the treatment conventional for MC simulations, we consider a basic rectangular configurational cell ($0 < X, Y < L$) with a finite number N of particles, which periodically repeats itself in the XY-directions.

Thus, the problem is to evaluate the Coulomb energy for a given configuration $\{\mathbf{r}_i\}$ of particles. The total energy of the system contains the contributions stemming from the interparticle interactions

$$V_{\rm Coul} = \frac{1}{2}\sum_{i=1}^{N}\sum_{j=1}^{N}\sum_{\mathbf{m}}^{\infty}{}' \frac{Q^2}{|\mathbf{r}_i - \mathbf{r}_j + L\mathbf{m}|} \tag{1}$$

taking account of the interactions with the infinite array of repeating image cells, and the contributions $V_{\rm BG}$ associated with the presence of the uniform background.

Here the two-dimensional vector $\mathbf{m}$ with the integer components $m_x = 0, \pm 1, \ldots \pm\infty$; $m_y = 0, \pm 1, \ldots \pm\infty$ enumerates the cells in the array; $\mathbf{r}_i = (x_i, y_i, z_i)$ is the radius vector of the i-th particle, and the prime sign at the sum means that the term with $i = j$ and $m_x = m_y = 0$ should be omitted.

Straightforward calculations of sum (1) is impractical, since the series converges very slowly. Much more efficient approach for calculating the Coulomb sums is Ewald's technique adapted for quasi-$2D$ case. As is shown in [15], expression (1) can be split into a number of terms

$$V_{\rm Coul} = V_{\rm dir} + V_{\rm inv} + V_{0,\rm inv} - V_{\rm self}, \tag{2}$$

where

$$V_{\rm dir} = \frac{1}{2}\sum_{i}^{N}\sum_{j}^{N}\sum_{|m_x|,|m_y|\le 1}{}' \frac{Q^2 \mathrm{erfc}(\alpha|\mathbf{r}_i - \mathbf{r}_j + L\mathbf{m}|)}{|\mathbf{r}_i - \mathbf{r}_j + L\mathbf{m}|}, \tag{3}$$

$$V_{\rm inv} = \frac{\pi}{L^2}\sum_{i}^{N}\sum_{j}^{N}\sum_{|\mathbf{q}|\neq 0}\frac{Q^2}{q} e^{qz_{ij}}\,\mathrm{erfc}\left(\frac{q}{2\alpha} + \alpha z_{ij}\right) \times$$

$$\times \cos(\mathbf{q}\mathbf{u}_{ij}), \tag{4}$$

$$V_{0,\rm inv} = -\frac{\sqrt{\pi}}{\alpha L^2}\sum_{i,j} Q^2\left[e^{-\alpha^2 z_{ij}^2} + \alpha z_{ij}\sqrt{\pi}\,\mathrm{erf}(\alpha z_{ij})\right], \tag{5}$$

$$V_{\rm self} = \alpha N Q^2/\sqrt{\pi}. \tag{6}$$

Here, α is the so-called splitting parameter which determines the relative contributions of the sums in the direct and inverse spaces; $\mathbf{q} = 2\pi\mathbf{n}/L$ are the $2D$ wave vectors ($n_{x,y} = 0, \pm 1, \ldots \pm\infty$), over which the sums in the inverse $2D$ space are calculated; $\mathbf{u}_{ij} = \mathbf{u}_i - \mathbf{u}_j$ with $\mathbf{u}_i = (x_i, y_i)$ being the $2D$ radius vector of the i-th particle; $z_{ij} = z_i - z_j$.

Expression (3) is the fast converging sum in the direct $3D$ space which is taken only over those particles in adjacent cells, for which the difference in any of three coordinates does not exceed a certain maximal cutoff length $L_{\rm max}$; expressions (4) and (5) represent the sums in the inverse $2D$ space.

In a way quite similar to that employed in [15] for the evaluation of the zero-th component of the energy $V_{0,\rm inv}$ in the inverse space, one can obtain the interaction with the uniform background (BG) (assuming the particles to reside *within* the immobile background and omitting the irrelevant constants) in the form

$$V_{\rm BG} = \frac{\pi N Q^2}{2L^2 H}\sum_{i=1}^{N} z_i^2. \tag{7}$$

Thus, the above expressions were employed in the present MC simulations to calculate the total configurational energy $V_{\rm tot} = V_{\rm Coul} + V_{\rm BG}$ of $1D$-confined OCP.

2. Monte Carlo Simulations

The state of $1D$-confined OCP can be unambiguously specified by the two quantities, the dimensionless width $h = 2H/d$ and the coupling $\Gamma = e^2/k_{\rm B}Td$. The quantity $d = L/\sqrt{\pi N}$ has the meaning of the average interparticle distance and is used throughout this paper as the length unit. Let us mention that, in the case of one layer in the system, the quantities d and Γ coincide with ones defined for strictly $2D$ systems, whereas, in the case of K layers, they differ from the relevant intralayer parameters by the factor $\simeq \sqrt{K}$. Note that the interaction with the uniform background (rewritten in the dimensionless form)

$$\frac{V_{\rm BG}}{k_{\rm B}T} = \frac{\Gamma}{h}\sum_{i=1}^{N}\tilde{z}_i^2, \tag{8}$$

can be viewed as a confining oscillator field in Z-dimension (here, $\tilde{z} = z/d$). In what follows, we regard this expression as the one including both effects of neutralizing background and the additional external oscillator fields, i.e., the width parameter h relates to the overall confining field.

The structure is studied in terms of $2D$ radial intra- and interlayer pair distribution functions and the bond-orientational order parameter for $2D$ m-fold symmetry [16]

$$O_m = \left\langle \left| \frac{1}{N_L}\sum_l \Psi_l \right| \right\rangle, \tag{9}$$

where

$$\Psi_l = \frac{1}{m}\sum_k \exp(im\theta_{lk}), \tag{10}$$

N_L is the number of particles within the layer, and θ_{lk} is the angle between the bond connecting the l-th particle with its nearest neighbours and some fixed axis.

The sum in (10) is taken over the bonds connecting the l-th particle with all the nearest neighbours, i.e. the particles at the distance less than the first minimum $r_{\rm min}$ in the radial intralayer distribution function; the brackets $\langle\cdots\rangle$ denote the canonical averaging. The type of $2D$ symmetry within layers can be simply estimated by the average number of $2D$ nearest neighbours N_n, which is expected to be close to 4 or 6 for the square or hexagonal types of symmetry, respectively.

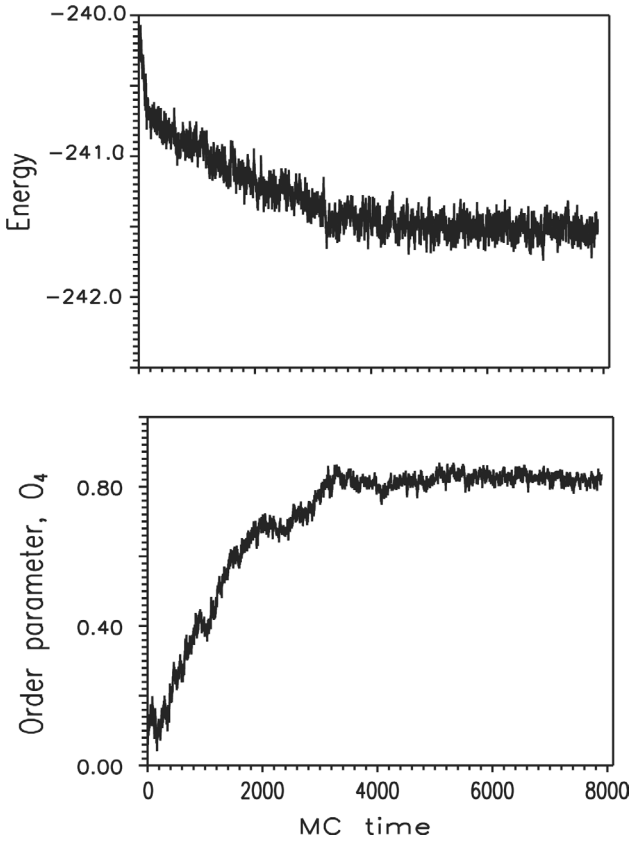

Fig.1. Freezing of $1D$-confined OCP to a two-layered crystal structure with the four-fold symmetry at $\Gamma = 220$ in MC simulations

MC simulations were carried out for the canonical (NVT) ensemble by using the conventional Metropolis algorithm [17] with the number of particles being within the range $N = 112 \div 390$. Computer simulations of strongly coupled Coulomb systems are difficult due to the well-known ergodicity problem. In other words, OCP tends to get trapped in glassy states, and, as a result, the equilibration time needed for the system to freeze into a crystal lattice is very long. In the present simulations, this time is, on average, $\simeq 10^7 - 10^8$ trial configurations. Another difficulty is that the difference in the average energies between the crystal and the glassy disordered states is rather small for the range $\Gamma = 300 \div 800$, on the order $\simeq 10^{-4}$. This necessitates high precision calculations of the configurational energy. In these simulations, the relative error in the calculation

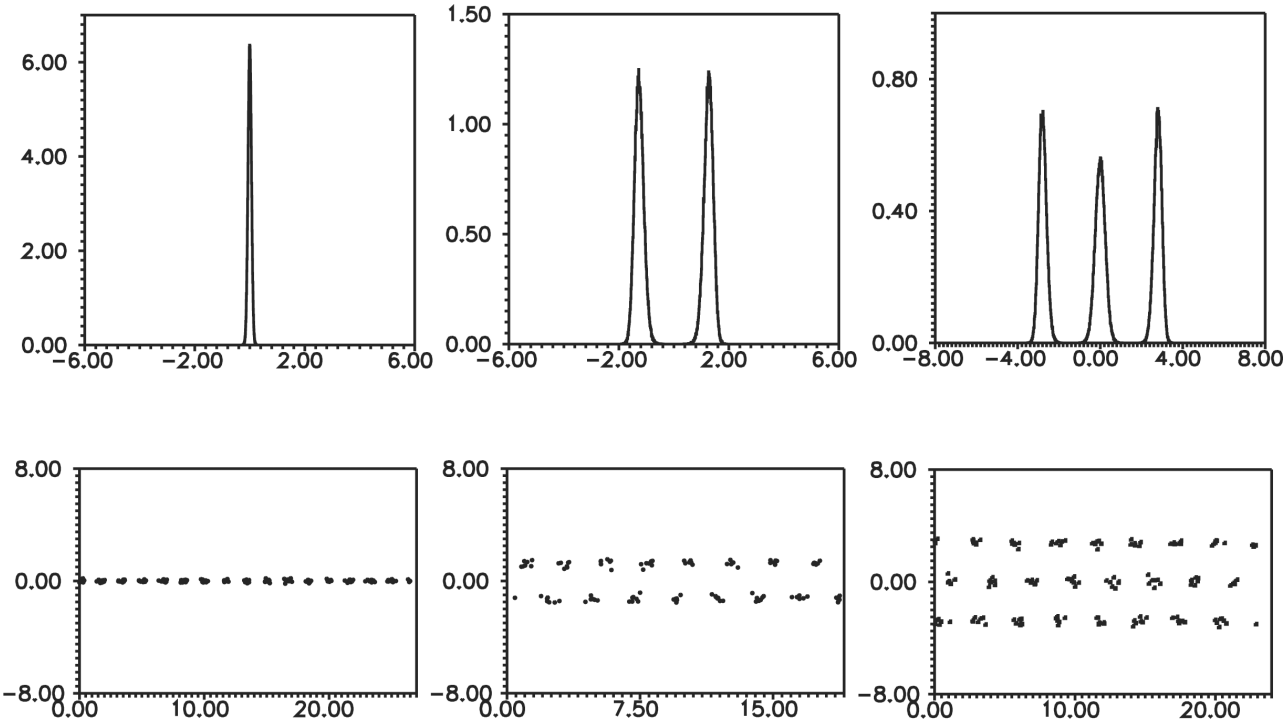

Fig.2. Layered structures in $1D$-confined OCP, $\Gamma = 300$. Top: transverse probability (density) distributions; bottom: side view of equilibrium MC configurations. The width is increasing from the left to the right: $h = 0.78;\ 2.53;\ 4.21$

of the Coulomb energy was controlled to be less than 10^{-6}, which was achieved by using the appropriate number of wave vectors in the inverse space and the values of the splitting parameter in computations of $2D$ Ewald sums. Each computer run started from a randomly generated initial configuration. After reaching the equilibrium, every N-th configuration of the MC chain was assumed to be statistically independent and added to the canonical ensemle. In most of the simulations, the canonical averaging was performed over $\simeq$ 2000–10000 statistically independent configurations. An example of the typical behavior of the system during relaxation (freezing) is displayed in Fig.1. The equilibrium is associated with the steady average energy, and the ordered state can be detected by the considerable steady magnitude of the order parameter for a long MC time.

3. Results of Numerical Simulations

MC simulations were performed for the range of parameters $\Gamma = 300 \div 800$, $h = 0.02 \div 4.8$, which correspond to the crystal structures with the number of layers $K = 1 \div 3$. The results are presented in figures and the table.

In Fig.2, the transversal probability distributions are displayed as a function of the width h. As is seen from the figure, with increasing the width parameter, the system undergoes transitions from one- to two-layered and from two- to three-layered structures. These transitions occur at the points $h \simeq 1.1$ and $h \simeq 2.9$, respectively.

One of the most interesting results is a series of transitions in the internal structure of the layers occuring with increasing the width of the system, Fig.3. The structure obtained for one-layered systems is well-known, it is a simple hexagonal lattice quite similar to that observed in strictly $2D$ case [8, 9]. Just above the point $h = 1.1$, the system crystallizes in a two-layered square structure, which is a feature of a BCC lattice in {100} plane. With increasing the width, above the point h =1.8, the system undergoes a transition to a hexagonal FCC {111} structure with the same number of layers $K = 2$. The associated changes in the intra- and interlayer distribution functions can be seen in Fig.4. The type of symmetry can be determined (along with visual observations) by the comparison with radial distributions of ideal BCC and FCC lattices, and by the position of the first minimum in the intralayer distribution function, which moves from 3.0 to 3.6 with increasing the width. Accordingly, the computed number

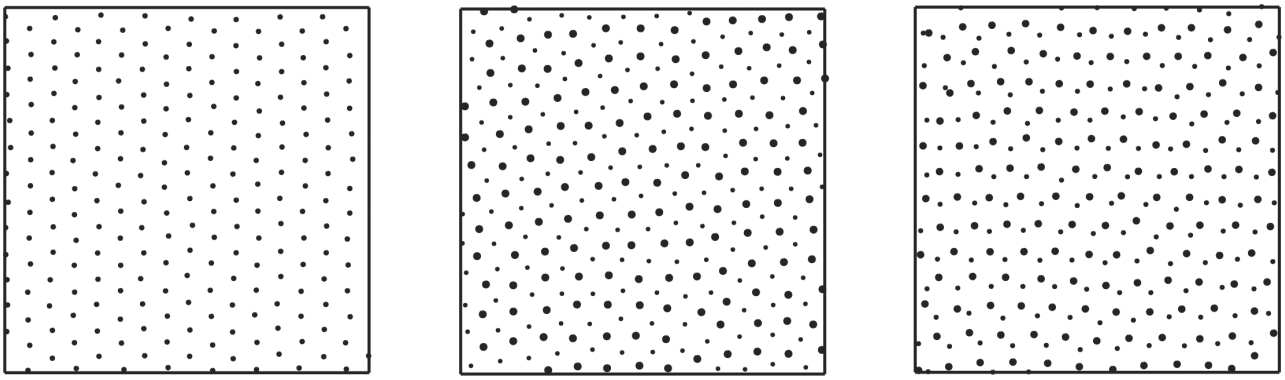

Fig.3. Equilibrium MC configurations of $1D$-confined OCP, $\Gamma = 500$. From the left to the right: one-layered hexagonal lattice, $h = 0.5$; two-layered square lattice BCC{100}, $h = 1.28$; two-layered hexagonal lattice FCC{111}, $h = 2.65$. Points and larger circles indicate the positions of particles in different layers

Structural properties of layered systems obtained in MC simulations

h	Γ	K	S	N_c	N_n	O_4	O_6	D	N
		1	triangles	6			1.00*		
0.02	300				6.00		0.88		224
0.5	300				6.00		0.88		224
	500				6.00		0.93		224
		2	BCC{100}	4		1.00*		0.50*	
1.28	300				3.96	0.90		0.41	288
	500				3.98	0.94		0.41	288
1.45	300				4.06	0.84		0.52	288
1.62	300				4.16	0.80		0.62	288
	500				4.00	0.90		0.61	288
		2	FCC{111}	6			1.00*	0.82*	
2.42	300				6.00		0.82	0.90	390
	500				6.00		0.90	0.90	390
2.74	300				6.00		0.80	1.04	112
	500				6.00		0.90	1.05	112
		3	BCC{100}	4		1.00*		0.50*	
3.13	500				4.18	0.82		0.67	192
		3	BCC{110} (rhombic)	4		0.78*		0.82*	
3.65	500				4.41	0.65		0.77	192
		3	FCC{111}	6			1.00*	0.82*	
4.26	500				6.00		0.88	0.87	168
		3	HCP	6			1.00*	0.82*	
4.26	500				6.00		0.87	0.87	168

N o t e. h — width parameter, Γ — coupling parameter, K — number of layers, S — structure, N_c — $2D$ coordination number, N_n — average number of $2D$ nearest neighbours, O_4/O_6 — orientational order parameter for four/six-fold symmetry, N — number of particles in MC cell, D — ratio of the interlayer to the lattice spacing (defined by the first maximum in the relevant radial distributions). The values marked with the asterisk relate to the 'ideal' lattices. The absolute error in the computations of the order parameters does not exceed 0.016.

of the nearest $2D$ neighbours increases therewith from $N_n = 4$ to $N_n = 6$.

The range $h = 1.5 \div 1.8$ can be regarded as the region of transition, where the behavior of distributions gradually changes and BCC{100} lattice acquires large-scale deformations. This is reflected by some decrease in the order parameter O_4.

A similar transition from the square to hexagonal structure is observed in three-layered systems within the range $h = 2.9 \div 4.8$, Fig.5. Note that, at wider interlayer separations, two competing hexagonal structures are observed, FCC{111} and HCP, as dependent on initial random configurations. The average energies obtained in simulations for these structures are equal (with accuracy of these MC simulations). Since the lattices HCP and FCC{111} differ only by the arrangement of the third layer (the former has the order of layers $ABABAB...$ and the latter has $ABCABCABC...$), it means that the structure type is determined by the interactions between the nearest layers only (i.e., the interaction between the outer layers is insignificant).

The intermediate deformed square lattice consisting of elongated hexagons (or elongated squares) is better defined in this case and can be regarded as the same BCC structure in {110} orientation, or, more generally, as a rhombic lattice.

Some information related to a number of selected runs is summarized in the table. As is seen from it, the interlayer spacing may considerably deviate from the corresponding 'ideal' values, so that the terms 'BCC' and 'FCC' lattice used throughout this paper apply to intra- and interlayer correlations rather than to the $3D$ structure as a whole.

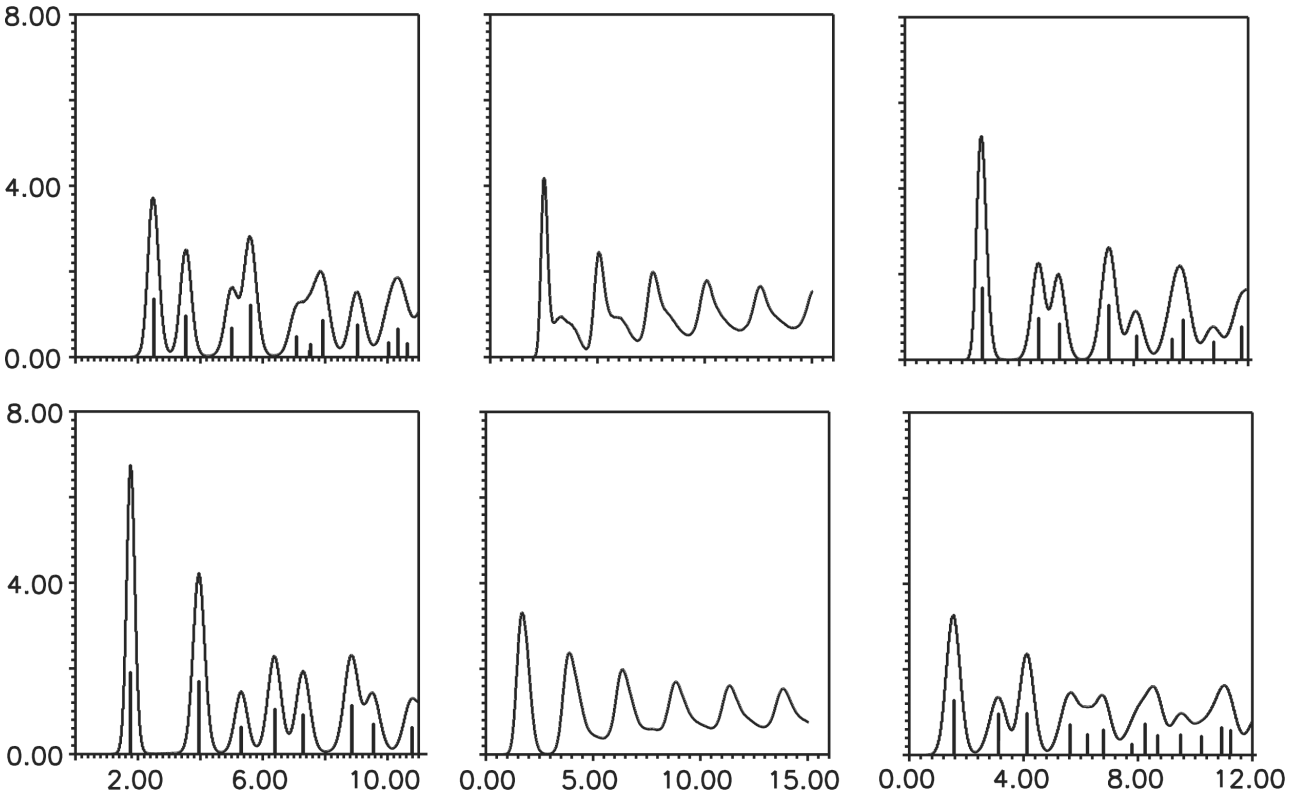

Fig.4. Radial $2D$ intralayer (top) and interlayer (bottom) distributions for two-layered structures at $\Gamma = 400$ as dependent on the width parameter. From the left to the right: $h = 1.28,\ 1.71,\ 2.42$. The vertical impulses relate to the ideal BCC{100} (left) and FCC{111} (right) lattices

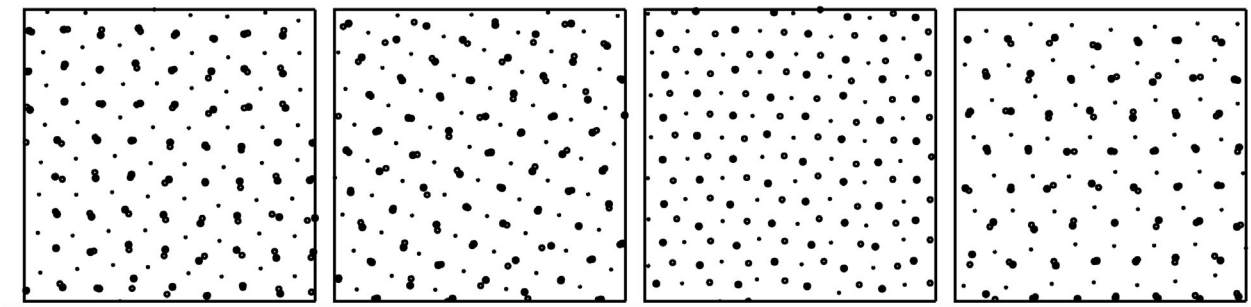

Fig.5. Equilibrium MC configurations for three-layered structures for $\Gamma = 500$. From the left to the right: BCC{100}, $h = 3.13$; BCC{110} (rhombic), $h = 3.38$; FCC{111}, $h = 4.26$; HCP, $h = 4.26$. The positions of particles are marked with points (the inner layer) and larger circles (outer layers)

The MC simulations performed for the range $\Gamma = 300 \div 800$ resulted in similar structural properties, except that the peaks in the radial distributions are broader for higher temperatures. It should be pointed out that only 5–10% of MC runs starting from randomly generated initial configurations result in perfect lattices given in the figures. In the rest of the cases, the system gets stuck in the states with lower symmetry or in the defect lattices, especially, for a larger number of particles. The above-presented structures are accepted as the final equilibrium ones, since i) they are formed spontaneously, as a result of the relaxation of the system to the thermodynamical equilibrium, ii) they have the lowest average energy, and iii) inverse spontaneous relaxation to metastable states with lower symmetries and higher energies is never observed.

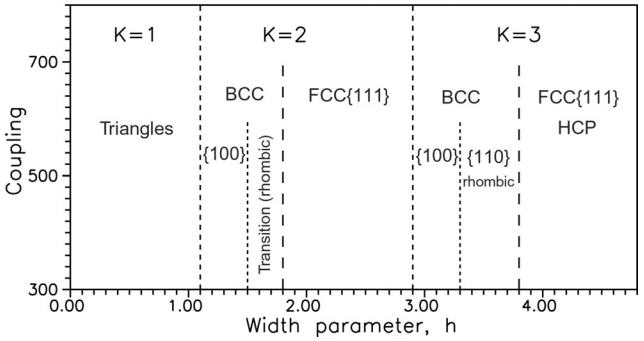

Fig.6. Crystal structure for $1D$-confined strongly coupled OCP obtained in MC simulations

Conclusions

Thus, the MC simulations of strongly coupled OCP confined in quasi-$2D$ geometry reveal a series of structural transitions with alternating square (BCC{100} or BCC{110}) and hexagonal (FCC{111} or HCP) symmetries, which occur with increasing the width of the system. The relevant diagram for the anticipated crystal structure within the range $\Gamma = 300 \div 800$ is presented in Fig.6. Note the good correlation of the results obtained with the experimental observations of similar transitions in $1D$-confined charged colloids [1] and planar ion structures in Penning traps [13], as well as the results of computer simulations of $1D$-confined hard spheres [12]. This indicates that the structural transitions under consideration are the rather general properties of systems with repulsive forces confined in quasi-$2D$ geometry.

1. *Murray C.A., Van Winkle D.H.*//Phys.Rev.A.— 1986.— **64**.— P.562.
2. *Thomas H., Morfill G.E., Demmel V., Goree J., Feuerbacher B., Möhlmann D.*//Phys.Rev.Lett.— 1994.— **73**.— P.652.
3. *Fowler A.B., Stern F.*//Rev.Mod.Phys.— 1982.— **54**.— P.437.
4. *Kalman G.J., Donko Z., Golden K.I.*//Contrib.Plasma Phys.— 2001.— **41**.— P.191.
5. *Hanna C.B., Haas D., Diaz-Velez J.C.*//Phys.Rev.B.— 2000-II.— **61**, P.13882.
6. *Pollock E.L., Hansen J.P.*//Phys.Rev.A.— 1973.— **8**.— P.3110.
7. *Brush S.G., Sahlin H.L., Teller E.*//J.Chem.Phys.— 1966.— **45**.— P.2102.
8. *Gann R.C., Chakravarty S., Chester G.V.*//Phys.Rev.B.— 1979.— **B20**.— P.326.
9. *Morf R.H.*//Phys.Rev.Lett.— 1979.— **43**.— P.931.
10. *Grimes C.C, Adams G.*//Ibid.— 1979.— **42**.— P.795.
11. *Dubin D.H.E.*//Ibid.— 1993.— **71**.— P.2753.
12. *Pansu B., Pieransky Pi., Pieransky Pa.*//J.Phys.— 1984.— **45**, P.331.
13. *Mitchell T.B. et al.*//Science.— 1998.— **282**.— P.1290.
14. *Schiffer J.P.*//Phys.Rev.Lett.— 1988.— **61**.— P.1843.
15. *Bystrenko O.V.*//Phys.Rev.E.— 2002.— **65**.— P.037702.
16. *Zippelius A., Halperin B.I., Nelson D.R.*//Phys.Rev.B.— 1990.— **B22**.— P.2514.
17. *Monte Carlo* Methods in Statistical Physics (Edited by K. Binder).— Berlin: Springer, 1979.

Received 15.11.02

КРИСТАЛІЧНА СТРУКТУРА СИЛЬНОЗВ'ЯЗАНОЇ ОДНОКОМПОНЕНТНОЇ ПЛАЗМИ В КВАЗІДВОВИМІРНІЙ ГЕОМЕТРІЇ. МОДЕЛЮВАННЯ МЕТОДОМ МОНТЕ-КАРЛО

О. В. Бистренко

Р е з ю м е

Сильнозв'язана однокомпонента плазма досліджується методом комп'ютерних моделювань Монте-Карло. Структура шарів, виникаючих в такій системі, досліджена за допомогою двовимірних парних внутрішньошарових та міжшарових функцій розподілу і орієнтаційних параметрів порядку. Найсуттєвішим результатом є спостереження ряду структурних переходів з квадратною (об'ємоцентричною кубічною) та гексагональною (гранецентричною кубічною або гексагональною щільнопакованою) симетрією, які чергуються в залежності від відстані між шарами. Результати моделювань добре узгоджуються з експериментальними спостереженнями аналогічних переходів в одновимірнообмежених заряджених коллоїдах та в іонних структурах в пастках Пеннінга.

КРИСТАЛЛИЧЕСКАЯ СТРУКТУРА СИЛЬНОСВЯЗАННОЙ ОДНОКОМПОНЕНТНОЙ ПЛАЗМЫ В КВАЗИДВУМЕРНОЙ ГЕОМЕТРИИ. МОДЕЛИРОВАНИЕ МЕТОДОМ МОНТЕ-КАРЛО

А. В. Быстренко

Р е з ю м е

Сильносвязанная однокомпонентная плазма исследуется методом компьютерных моделирований Монте-Карло. Структура слоев, возникающих в такой системе, исследована с помощью двумерных парных внутрислойных и межслойных функций распределения и ориентационных параметров порядка. Наиболее значительным результатом является наблюдение ряда структурных переходов с чередующейся квадратной (объемоцентрической кубической) и гексагональной (гранецентрической кубической либо гексагональной плотноупакованной) симметрией, в зависимости от расстояния между слоями. Результаты моделирований хорошо согласуются с экспериментальными наблюдениями аналогичных переходов в одномерноограниченных заряженных коллоидах и в ионных структурах в ловушках Пеннинга.